Quantitative Systems Pharmacology Modeling of Mipasetamab Uzoptirine Integrates Knowledge and Defines Dosing Strategy for Patients With Sarcoma

Joseph Boni,[1] Yuezhe Li,[2] Timothy Knab,[2] Ilaria Conti,[1] George Shen,[1*] A. Katharina Wilkins[2]

[1]ADC Therapeutics, New Providence, NJ; [2]Metrum Research Group, Tariffville, CT

By employing PBPK-QSP modeling, dosing regimens can be evaluated to explore hypotheses for further clinical investigation

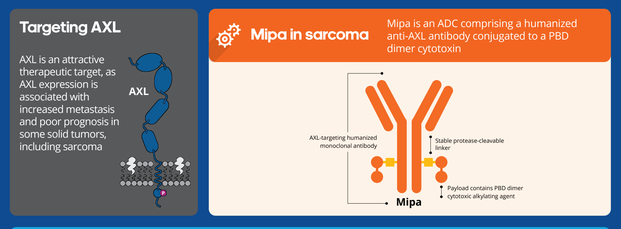

ADC, antibody–drug conjugate; IC_{50}, half maximal inhibitory concentration; Mipa, mipasetamab uzoptirine; obs; observed; PBD, pyrrolobenzodiazepine; PBPK-QSP, physiologically based PK quantitative systems pharmacology model; PK, pharmacokinetics; Q3W, every 3 weeks; sims, simulations.

Poster presented at the Connective Tissue Oncology Society (CTOS) Annual Meeting. November 13-16, 2024, San Diego, CA, USA

CONCLUSIONS

- The model predicted that a higher total dose (up to 19 mg, administered every 3 weeks [Q3W]) of ADCT-601 (mipasetamab uzoptirine; Mipa) resulted in a higher percentage of responders in patients with sarcoma
- Tumor proliferation rate, tumor perfusion, and tumor heterogeneity (i.e., the fraction of AXL$^+$ cells in the tumor) were predicted to be key factors that impacted predicted tumor volume reduction with Mipa treatment
- Soluble AXL (sAXL) in the plasma was predicted to have a minor impact on Mipa plasma pharmacokinetics (PK) and antitumor effect, likely due to Mipa plasma concentrations greatly exceeding sAXL levels

INTRODUCTION

- AXL overexpression is linked to high metastatic potential and chemotherapy resistance, consequently leading to poor overall survival in some solid tumors, including sarcoma and non–small cell lung cancer[1-3]
- Mipa is an antibody–drug conjugate (ADC) comprising a humanized anti-AXL antibody conjugated to a potent chemotherapeutic agent, SG3199 (pyrrolobenzodiazepine dimer cytotoxin), via a cleavable linker[4]
  - Mipa demonstrated antitumor activity in preclinical murine xenograft models of sarcoma, adenoid cystic carcinoma, and pancreatic cancer.[4-6] Further, Mipa showed promising clinical activity in patients with solid tumors in phase 1 trials[5,7]

OBJECTIVE

- To develop a model predicting the biodistribution and antitumor effect of Mipa for virtual patients with sarcoma following various dosing regimens

METHODS

Model Construction

- A novel physiologically based PK quantitative systems pharmacology model was developed to describe the effect of Mipa on sarcoma. The construct incorporated multiple literature-based model elements,[8] including physiologic tissue distribution and interstitial compartment disposition of IgG1-based ADC, ADC uptake, SG3199 release, and cell killing of the tumor cells (**Figure 1**)

Figure 1. PBPK-QSP Model for Mipa

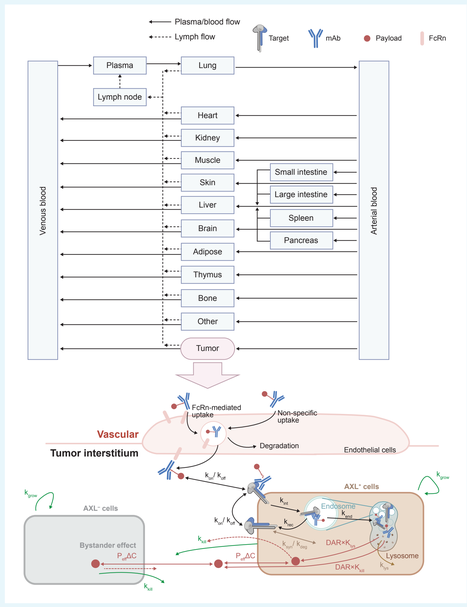

ADC, antibody–drug conjugate; DAR, drug-antibody ratio; FcRn, IgG receptor; K_{deg}, degradation rate for surface AXL; K_{end}, endosomes to lysosomes ADC transport rate; K_{grow}, growth rate for tumor cells; K_{int}, internalization rate for surface AXL; K_{ys}, rate of payload-induced cell killing; K_{ys}, ADC lysosomal degradation rate; K_{off}, off-rate for ADC binding to AXL; K_{on}, on-rate for ADC binding to AXL; K_{rec}, AXL recycling rate from endosomes to the cell surface; K_{syn}, synthesis rate for surface AXL; mAb, monoclonal antibody; Mipa, mipasetamab uzoptirine; PBPK-QSP, physiologically based PK quantitative systems pharmacology; $P_{eff}\Delta C$, payload diffusion out of AXL$^+$ cells and into AXL$^-$ cells (driven by concentration gradient); PK, pharmacokinetics.

- Key assumptions were the following:
  - AXL$^+$ cells only existed in the tumor
  - Inside the tumor, all AXL$^+$ cells were assumed to have the same AXL expression level, while all AXL$^-$ cells were assumed to have no AXL expression
  - AXL$^+$ and AXL$^-$ cells were assumed to be well mixed in the tumor
  - Unbound SG3199 was assumed to be diffusing from AXL$^+$ cells to the tumor interstitium and then to AXL$^-$ cells, but unbound SG3199 did not diffuse into or out of the tumor
  - ADC deconjugation in plasma was assumed to be negligible
  - Tumor perfusion was assumed to be the only parameter that impacted ADC penetration into the tumor (i.e., this model did not explicitly include a penalty for larger tumor size)
  - sAXL was not included in the base model, but sensitivity analyses (data not shown) were performed and sAXL was projected to have a limited impact on the antitumor effect of Mipa
  - The tumor was assumed to be a sphere; classification of partial response was based on 30% reduction in tumor diameter (i.e., 66% reduction in tumor volume)
- In vitro parameters (e.g., receptor dynamics and ADC-induced cell death) were parameterized based on literature values or optimized based on preclinical data (**Table 1**)
  - PK parameters were fit to clinical PK data
  - The following 4 parameters were selected to vary in sarcoma virtual patient grid scans
    - Tumor doubling time
    - Surface AXL copy per AXL$^+$ cell
    - AXL$^+$ fraction
    - Tumor perfusion

Table 1: Parameters for Mipa In Vitro Model

Parameter name	Description	Reference	Value
Variable parameters			
R_{copies}	AXL copy number on AXL$^+$ cells	Mavrangelos et al.[9]	1k, 2k, 5k, 10k, 20k, 50k, 100k
K_{grow}	Growth rate for tumor cells	Calculated based on tumor doubling time (20, 30, or 40 days)	0.0014 h^{-1}, 0.00096 h^{-1}, 0.00072 h^{-1}
AXL$^+$ fraction	The fraction of AXL$^+$ cells in the tumor at the beginning of treatment	Flem-Karlsen et al.[10]	0.1, 0.2, 0.3, 0.4, 0.5, 0.6, 0.7, 0.8, 0.9, 1.0
Tumor perfusion (L/h/L)	Blood perfusion rate through the tumor	Soni et al.[11]	20, 25, 30
Constant parameters			
DAR	Drug-antibody ratio	Zammarchi et al.[4]	1.8
K_d	ADC-AXL binding affinity	Zammarchi et al.[4]	0.311 nM
K_{on}	On-rate for ADC binding to AXL	Optimized based on preclinical data	2.07 $nM^{-1}{\cdot}h^{-1}$
K_{off}	Off-rate for ADC binding to AXL	–	$K_{on}{\cdot}K_d$
K_{syn}	Synthesis rate for surface AXL	Optimized based on preclinical data	0.02 $nmol{\cdot}h^{-1}$
K_{deg}	Degradation rate for surface AXL	Bae et al.[12]	0.693 h^{-1}
K_{int}	Internalization rate for surface AXL	Optimized based on preclinical data	9.02 h^{-1}
K_{end}	Endosomes to lysosomes ADC transport rate	Hopkins et al.[13]	5.54 h^{-1}
K_{ys}	ADC lysosomal degradation rate	Hopkins et al.[13]	5.54 h^{-1}
K_{rec}	AXL recycling rate from endosomes to the cell surface	Optimized based on preclinical data	0.187 h^{-1}
K_{rec_AR}	ADC-AXL complex recycling rate from endosomes to the cell surface	Optimized based on preclinical data	2.43 h^{-1}
P_{eff}	Membrane permeability	Ogitani et al.[14]	12.2E–6 cm^2
E_{max} payload	Maximum killing efficiency induced by SG3199 inside cells	Optimized based on preclinical data	0.0099 h^{-1}
τ	Delayed cell death	Caimi et al.[15]	1 h
k_PL	SG3199 clearance in the tumor interstitium	Optimized based on preclinical data	0.04 h^{-1}
PS_K_d	Equilibrium binding constant for ADC to nonspecific cell membrane sites, governing PBPK tissue-specific clearance	Optimized based on PK data	0.01 µM
K_{d_6WT}	Equilibrium binding constant for ADC to FcRn, governing PBPK tissue-specific distribution and clearance	Optimized based on PK data	145 nM

ADC, antibody–drug conjugate; FcRn, IgG receptor; Mipa, mipasetamab uzoptirine; PBPK, physiologically based PK model; PK, pharmacokinetics.

RESULTS

- Modeling results indicated that more than 50% of patients with tumors >40% AXL$^+$ were predicted to achieve either a complete or partial response when Mipa was dosed at 13 mg Q3W (**Figure 2A**)
- When explored at a higher dose, Mipa was predicted to achieve over 50% responders when AXL$^+$ cell fraction was >20% and Mipa was dosed at 19 mg Q3W (**Figure 2B**)
  - Additionally, the model indicated that above a certain threshold (10k per AXL$^+$ cell at 13 mg Q3W; 2.5K per AXL$^+$ cell at 19 mg Q3W), the likelihood of response did not continue to increase

Figure 2. Predicted Responder Percentage in Populations With Varying AXL Expression per Positive Cell and Fraction of AXL$^+$ Cells With Mipa Dosages of (A) 13 mg Q3W and (B) 19 mg Q3W

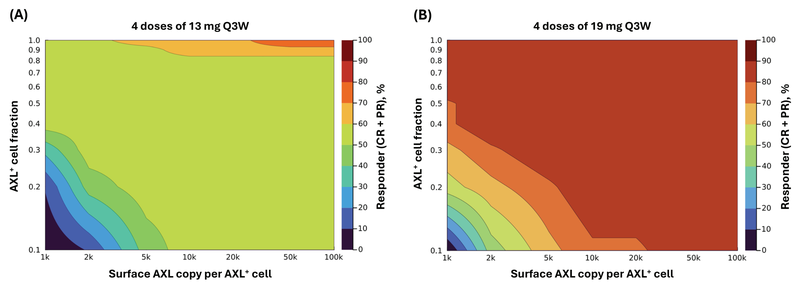

CR, complete response; Mipa, mipasetamab uzoptirine; PR, partial response; Q3W, every 3 weeks.

- Modeling results predicted that a fractionated dose interval or high induction dose followed by maintenance were predicted to promote sarcoma volume reduction in tumors with varying AXL expression (**Figure 3**)

Figure 3. Model-Predicted Tumor Control Comparing the Effects of Mipa Administration of 11 mg Q3W Versus Dose Fractionation Versus High Induction/Maintenance

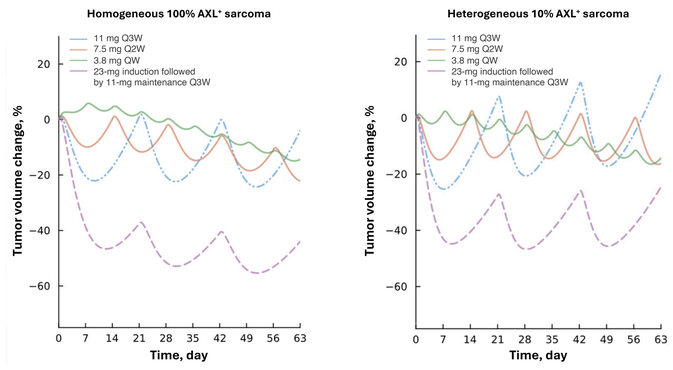

Model variables: induction dose = 23 mg, 1 cycle, Q3W; maintenance dose = 11 mg, 2 cycles, Q3W; tumor doubling time = 20 days; normalized tumor perfusion = 25 L/h/L. Left panel: 100% AXL$^+$ cells, 1,000 surface AXL per AXL$^+$ cell; right panel: 10% AXL$^+$ cells, 10,000 surface AXL per AXL$^+$ cell.
Mipa, mipasetamab uzoptirine; QW, every week; Q2W, every 2 weeks; Q3W, every 3 weeks.

- Simulation of various dosing regimens, including fixed Q3W dosing and a high induction dose followed by maintenance, suggested that dosing Mipa at higher levels would result in a higher percentage of responders (**Figure 4**)

Figure 4. Predicted Response by Total Dose of Mipa for Q3W and High Induction/ Maintenance Dosing at Various Levels for (A) Sarcoma Ranging From 10% to 100% AXL$^+$ Cells and (B) Sarcoma With ≥50% AXL$^+$ Cells

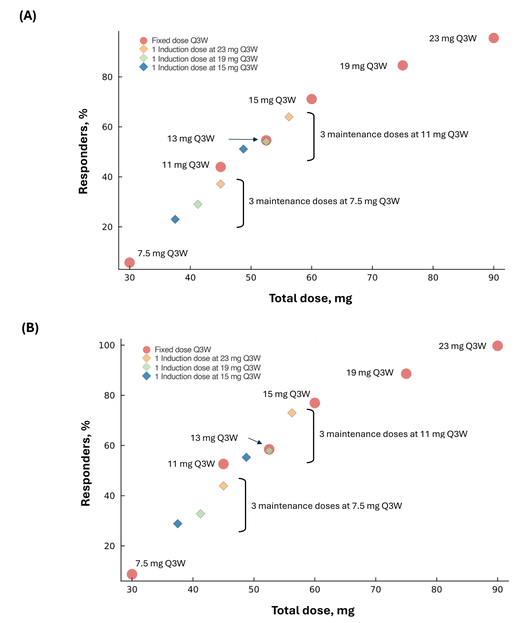

Mipa, mipasetamab uzoptirine; Q3W, every 3 weeks.

- Other simulations predicted that the sarcoma proliferation rate was a key driver for differential tumor shrinkage (data not shown) and that increasing concentrations of sAXL did not substantially impact Mipa concentration in the plasma or tumor volume change (data not shown)

Limitations

- A limitation of the constructed model is that it focused solely on efficacy. Translating efficacious dosage levels from virtual populations to clinical populations can be complicated by safety considerations that were not within the scope of this QSP model
- Although the model can be used to predict the efficacy of different dosing schemes, the model does not account for the clinical feasibility of administering different doses, such as Q3W administration versus QW administration

Acknowledgments

The analysis was funded by ADC Therapeutics SA and partially funded by Sobi. Medical writing and editorial support, provided by Citrus Scientific, a Citrus Health Group, Inc., company (Chicago, Illinois), was provided in accordance with Good Publication Practices (GPP 2022) and funded by ADC Therapeutics SA and Sobi.

Disclosures

J Boni: was an employee of ADC Therapeutics at the time of the study and is a current equity holder of ADC Therapeutics SA. **Y Li:** employee of Metrum Research Group. **T Knab:** employee of Metrum Research Group. **I Conti:** was an employee of ADC Therapeutics at the time of the study and currently holds equity/stock options at ADC Therapeutics SA, AstraZeneca, and Eli Lilly and Company. **G Shen:** employee of ADC Therapeutics and current equity holder of ADC Therapeutics SA. **AK Wilkins:** employee of Metrum Research Group.

Contact information

*George Shen: george.shen@adctherapeutics.com

References

1. Chen H, et al. *Cancer Treat Rev*. 2016;43:8-18.
2. Schoumacher M and Burbridge M. *Curr Oncol Rep*. 2017;19(3):19.
3. Zaman A and Bivona TG. *Lung Cancer (Auckl)*. 2021;12:67-79.
4. Zammarchi F, et al. *Mol Cancer Ther*. 2022;21(4):582-593.
5. Tolcher AW, et al. Presented at: European Society for Medical Oncology Congress (ESMO); Sep 26-30, 2019; Barcelona, Spain.
6. Humtsoe JO, et al. Presented at: Association for Cancer Research Annual Meeting; 2022; Philadelphia, PA.
7. Van Tine BA, et al. Presented at: American Association for Cancer Research (AACR) Annual Meeting; April 5-10, 2024; San Diego, CA.
8. Jones HM, et al. *CPT Pharmacometrics Syst Pharmacol*. 2019;8(10):738-747.
9. Mavrangelos C, et al. *J Immunol Methods*. 2004;289(1-2):169-178.
10. Flem-Karlsen K, et al. *PLoS One*. 2020;15(1):e0227187.
11. Soni S, et al. *Int J Hyperthermia*. 2015;31(6):615-625.
12. Bae SY, et al. *Oncotarget*. 2015;6(12):10146-10160.
13. Hopkins CR and Trowbridge IS. *J Cell Biol*. 1983;97(2):508-521.
14. Ogitani Y, et al. *Cancer Sci*. 2016;107(7):1039-1046.
15. Caimi PF, et al. *eJHaem*. 2024;5(1):76-83.